Anal. Chem. **2004,** *76,* 40−47

Discrimination of Bacteria Using Surface-Enhanced Raman Spectroscopy

Roger M. Jarvis and Royston Goodacre*

Department of Chemistry, UMIST, P.O. Box 88, Sackville Street, Manchester M60 1QD, U.K.

Raman spectroscopy has recently been shown to be a potentially powerful whole-organism fingerprinting technique and is attracting interest within microbial systematics for the rapid identification of bacteria and fungi. However, while the Raman effect is so weak that only ~1 in 10^8 incident photons are Raman scattered (so that collection times are in the order of minutes), it can be greatly enhanced (by some 10^3−10^6-fold) if the molecules are attached to, or microscopically close to, a suitably roughened surface, a technique known as surface-enhanced Raman scattering (SERS). In this study, SERS, employing an aggregated silver colloid substrate, was used to analyze a collection of clinical bacterial isolates associated with urinary tract infections. While each spectrum took 10 s to collect, to acquire reproducible data, 50 spectra were collected making the spectral acquisition times per bacterium ~8 min. The multivariate statistical techniques of discriminant function analysis (DFA) and hierarchical cluster analysis (HCA) were applied in order to group these organisms based on their spectral fingerprints. The resultant ordination plots and dendrograms showed correct groupings for these organisms, including discrimination to strain level for a sample group of *Escherichia coli*, which was validated by projection of test spectra into DFA and HCA space. We believe this to be the first report showing bacterial discrimination using SERS.

There is a continuing requirement for rapid, accurate, and preferably automated methods for the identification of microorganisms, particularly within the clinical environment. Ideal techniques for rapid microbial characterization would include those that require minimal sample preparation, permit the automatic analysis of many serial samples with negligible reagent costs, allow their rapid characterization against a stable database, are easy to use, and can be operated under the control of a PC. With recent developments in analytical instrumentation, these requirements are being fulfilled by physicochemical spectroscopic methods, often referred to as "whole-organism fingerprinting"[1,2] and more recently "metabolic fingerprinting".[3] Methods that have been attracting considerable interest are those based on mass spectrometry[4,5] and on the vibrational spectroscopic methods of Fourier transform infrared spectroscopy and Raman spectroscopy.[6−9]

Raman spectroscopy is a versatile technique that has been used on bacterial slurries,[2] bacterial and fungal (micro)colonies,[7] and even single bacterial cells,[10] to obtain highly information-rich spectra. However, the Raman effect is particularly weak and typically only ~1 in 10^8 incident photons are inelastically scattered; thus, collection times are on the order of minutes rather than seconds even when high laser power is used. The inelastic light-scattering process can be enhanced when the laser is within the molecular absorption bands of the sample. Excitation of this type is in resonance with the electronic transition and yields Raman scattering that is resonance enhanced.[11] Although deep UV resonance Raman (UVRR) has been used to analyze bacteria,[12] because of the high light energies involved photochemical effects cause sample degradation, which creates challenges in sample preparation. Moreover, UVRR is selective because only certain chromophoric segments of macromolecules absorb UV light.

By contrast, enhancements of some 10^3−10^6-fold (compared with the normal Raman scattering process) can be achieved using the method of surface-enhanced Raman scattering (SERS),[13] and even enhancements of up to 10^{15} have been reported for certain chemical species.[14] In addition to signal enhancement, SERS has a fluorescence-quenching effect,[15] and this is extremely useful when examining microorganisms, which often exhibit a high fluorescence background under excitation in the near-infrared to

* Corresponding author: (telephone) +44 (0)161 200 4480; (fax) +44 (0)161 200 4519; (e-mail) R.Goodacre@umist.ac.uk.

(1) Magee, J. T. In *Handbook of New Bacterial Systematics*; Goodfellow, M., O'Donnell, A. G., Eds.; Academic Press: London, 1993; pp 383−427.
(2) Goodacre, R.; Timmins, É. M.; Burton, R.; Kaderbhai, N.; Woodward, A.; Kell, D. B.; Rooney, P. J. *Microbiology* **1998**, *144*, 1157−1170.
(3) Fiehn, O. *Plant Mol. Biol.* **2002**, *48*, 155−171.
(4) Lay, J. O. *Trends Anal. Chem.* **2000**, *19*, 507−516.
(5) Vaidyanathan, S.; Rowland, J. J.; Kell, D. B.; Goodacre, R. *Anal. Chem.* **2001**, *73*, 4134−4144.
(6) Naumann, D.; Helm, D.; Labischinski, H. *Nature* **1991**, *351*, 81−82.
(7) Maquelin, K.; Choo-Smith, L.-P.; van Vreeswijk, T.; Endtz, H. P.; Smith, B.; Bennett, R.; Bruining, H. A.; Puppels, G. J. *Anal. Chem.* **2000**, *72*, 12−19.
(8) Maquelin, K.; Choo-Smith, L. P.; Endtz, H. P.; Bruining, H. A.; Puppels, G. J. *J. Clin. Microbiol.* **2002**, *40*, 594−600.
(9) Maquelin, K.; Kirschner, C.; Choo-Smith, L.-P.; van den Braak, N.; Endtz, H. P.; Naumann, D.; Puppels, G. J. *J. Microbiol. Methods* **2002**, *51*, 255−271.
(10) Schuster, K. C.; Reese, I.; Urlaub, E.; Grapes, R.; Lendl, B. *Anal. Chem.* **2000**, *72*, 5529−5534.
(11) Asher, S. A. *Anal. Chem.* **1993**, *65*, 59A−66A.
(12) Nelson, W. H.; Manoharan, R.; Sperry, J. F. *Appl. Spectrosc. Rev.* **1992**, *27*, 67−124.
(13) Moskovits, M. *Rev. Mod. Phys.* **1985**, *57*, 783−826.
(14) Nie, S. M.; Emery, S. R. *Science* **1997**, *275*, 1102−1106.
(15) Kneipp, K.; Haka, A. S.; Kneipp, H.; Badizadegan, K.; Yoshizawa, N.; Boone, C.; Shafer-Peltier, K. E.; Motz, J. T.; Dasari, R. R.; Feld, M. S. *Appl. Spectrosc.* **2002**, *56*, 150−154.

10.1021/ac034689c CCC: $27.50
Published on Web 11/19/2003

visible regions of the electromagnetic spectrum. Moreover, since excitation is in this part of the electromagnetic spectrum there are no drawbacks associated with photochemical degradation of the sample. SERS has received much attention recently within biomedicine[16] and genomics[17] and is emerging as a very powerful (bio)chemical detection method.[18] Therefore, we believe SERS to be a sensitive analytical tool that can be used to study low concentrations of microbial biomass and provide information-rich spectra.

Several investigations into SERS of bacteria have been undertaken.[19−22] Zeiri et al.[19] performed SERS with a sodium borohydride-reduced silver colloid at 514.5-nm excitation. Perhaps surprisingly, they noted very little difference between SERS from the surface of chemically diverse Gram-positive and Gram-negative bacteria and attributed the spectra to the presence of one molecule, flavin adenine dinucleotide. Guzelian et al.[22] recently used a gold SERS substrate with 784-nm excitation to investigate the individual components of bacteria and concentrated on nucleic acids, amino acids, and peptides. These authors stated that SERS spectra obtained from bacteria under these conditions will take their major contribution from cell surface biochemistry, yet they did not analyze carbohydrates, which are frequently associated with the outer cell membrane. Since these studies only analyzed a handful of different bacteria, they fail to answer the question, "can SERS reliably *differentiate* between different bacteria?"

SERS relies on either the adsorption or close proximity of an analyte to a metal substrate.[23,24] The substrate can take the form of a roughened metal surface, a colloidal solution, or a roughened electrode. For the present study, an aggregated silver colloid was used. The total enhancement of the SERS effect is explained by two processes; a charge-transfer mechanism, known as *chemical enhancement*, and an *electromagnetic enhancement* effect. Chemical enhancement is thought to take place at sites of atomic-scale roughness on the metal surface and involves electronic coupling (an exchange of electrons) between the metal substrate and the analyte. Electromagnetic enhancement, thought to contribute more to the overall magnitude of enhancement, takes place on the nanometer scale and can be attributed to surface plasmon oscillations. These provide a higher "local" optical field, due to redistribution and concentration of electromagnetic energy. Coupled with the incoming electric field from the incident radiation, this generates a larger spectroscopic signal for an analyte "caught" in both fields. For colloidal SERS, the resonance frequency of the plasmon oscillations is dependent on the size and shape of the particles.[25]

The main challenge with SERS is the attainment of reproducible spectra, without which quantitative analysis is difficult. This is because the laser has to strike the sample at a point where the SERS substrate and analyte are both present and in the appropriate geometry. Moreover, the reproducibility of the metal substrates needs to be improved, although semiautomatic flow systems might provide a solution.[26]

Urinary tract infection (UTI) is a disease that affects millions of people across all age groups throughout the world.[27,28] The organisms most commonly found to be the cause of UTI are members of the family *Enterobacteriaceae*, particularly *Escherichia coli* which is the causal agent in >50% of cases, *Klebsiella* spp., and *Pseudomonas aeruginosa*. In addition to these, enterococci are also frequently connected with the disease (∼10% of cases).[29] Thus, the aim of the present study was to develop SERS as a rapid whole-organism fingerprinting method for the characterization of bacteria associated with UTI.

MATERIALS AND METHODS

Bacterial Strains and Growth Conditions. Clinical bacterial (n = 21) isolates from patients with UTI were obtained from Bronglais Hospital, Aberystwyth, as previously reported.[30] Identification by API20E (http://industry.biomerieux-usa.com/) biochemical tests showed the isolates to belong to *E. coli* (5 strains coded; Eco), *Klebsiella oxytoca* (2 strains coded; kox), *Klebsiella pneumoniae* (3 strains coded; kp), *Citrobacter freundii* (2 strains coded; Cf), *Enterococcus* spp. (4 strains coded; EntC), and *Proteus mirabilis* (5 strains coded; pm). All isolates were cultivated axenically and aerobically for 16 h at 37 °C on LabM blood agar base (IDG Plc, Lancashire, U.K.). After subculturing three times, biomass was carefully collected from single colonies using sterile plastic inoculating loops. These were then added to 4-μL aliquots of silver colloid with 2 μL of 0.01 M NaCl (99.9%, Fisher Scientific, Leicestershire, U.K.) aggregating agent, before spotting onto CaF_2 windows (Crystran Ltd., Dorset, U.K.).

In a further study to assess the discrimination of bacteria at the subspecies level, seven *E. coli* isolates (Eco11, Eco20, Eco31, Eco41, Eco42, Eco48, Eco49) were also cultured as detailed above.

Silver Colloid Preparation. Batches (n = 3) of citrate reduced silver colloid were prepared by a modified Lee and Meisel[31] method similar to that described by Munro et al.[32] All equipment (conical flask, mercury thermometer, magnetic stirrer) was thoroughly cleaned with detergent and then rinsed twice with distilled water. The conical flask containing 100 mL of distilled

(16) Kneipp, K.; Kneipp, H.; Itzkan, I.; Dasari, R. R.; Feld, M. S. *Curr. Sci.* **1999**, *77*, 915−924.
(17) VoDinh, T.; Stokes, D. L.; Griffin, G. D.; Volkan, M.; Kim, U. J.; Simon, M. I. *J. Raman Spectrosc.* **1999**, *30*, 785−793.
(18) Faulds, K.; Smith, W. E.; Graham, D.; Lacey, R. J. *Analyst* **2002**, *127*, 282−286.
(19) Zeiri, L.; Bronk, B. V.; Shabtai, Y.; Czege, J.; Efrima, S. *Colloids Surf. A* **2002**, *208*, 357−362.
(20) Efrima, S.; Bronk, B. V. *J. Phys. Chem. B* **1998**, *102*, 5947−5950.
(21) Fell, N. F.; Smith, A. G. B.; Vellone, M.; Fountain, A. W. In *Vibrational Spectroscopy-Based Sensor Systems*; Christesen, S. D., Sedlacek, A. J., III, Eds.; SPIE−International Society of Optical Engineering: Bellingham, WA, 2002; Vol. 4577, pp 174−181.
(22) Guzelian, A. A.; Sylvia, J. M.; Janni, J. A.; Clauson, S. L.; Spencer, K. M. In *Vibrational Spectroscopy-Based Sensor Systems*; Christesen, S. D., Sedlacek, A. J., III, Eds.; SPIE−International Society of Optical Engineering: Bellingham, WA, 2002; Vol. 4577, pp 182−192.
(23) Fleischmann, M.; Hendra, P. J.; McQuillan, A. J. *Chem. Phys. Lett.* **1974**, *26*, 163−166.
(24) Chang, R. K., Furtak, T. E., Eds. *Surface Enhanced Raman Scattering*; Plenum Press: New York, 1982.
(25) Kerker, M.; Wang, D. S.; Chew, H.; Siiman, O.; Bumm, L. A. In *Surface Enhanced Raman Scattering*, 1st ed.; Chang, R. K., Furtak, T. E., Eds.; Plenum Press: New York, 1982; Vol. 1, pp 109−128.
(26) Keir, R.; Sadler, D.; Smith, W. E. *Appl. Spectrosc.* **2002**, *56*, 551−559.
(27) Foxman, B.; Barlow, R.; D'Arcy, H.; Gillespie, B.; Sobel, J. D. *Ann. Epidemiol.* **2000**, *10*, 509−515.
(28) Wilkie, M. E.; Almond, M. K.; Marsh, F. P. *Br. Med. J.* **1992**, *303*, 1137−1141.
(29) Slack, R. C. B. In *Antimicrobial Chemotherapy*; Greenwood, D., Ed.; Oxford University Press: Oxford, U.K., 1995; pp 243−250.
(30) Kassama, Y.; Rooney, P. J.; Goodacre, R. *J. Clin. Microbiol.* **2002**, *40*, 2795−2800.
(31) Lee, P. C.; Meisel, D. *J. Phys. Chem.* **1982**, *86*, 3391−3395.
(32) Munro, C. H.; Smith, W. E.; Garner, M.; Clarkson, J.; White, P. C. *Langmuir* **1995**, *11*, 3712−3720.

Table 1. UV−Visible Spectroscopy Data Characterizing Three Batch Preparations of Colloidal Silver Solution (A−C)[a]

	A	B	C
λ_{max}	438	427	415
extinction	0.56	0.57	0.60
fwhh	158	138	111

[a] Batch C was used for the bacterial discrimination study. A larger value for the absorption maximum (λ_{max}) equates to a larger particle size, a lower value for the extinction indicates greater aggregation, and a larger full width at half-height (fwhh) indicates wider particle size distribution.

water and the magnetic stirrer was placed on a stirrer hot plate, the mercury thermometer was suspended in the water, and the flask opening was covered with aluminum foil to minimize loss of water through evaporation. With continuous stirring, the contents of the flask were brought to a temperature of 45 °C, at which point 18 mg of $AgNO_3$ (>99%, Sigma, Dorset, U.K.) suspended in 2 mL of distilled water was added. With further heating and stirring, the solution was brought to boiling point and 2 mL of 1% (w/v) trisodium citrate (99.66%, Fisher Scientific) introduced to the flask. The solution was boiled for 10 min with continuous stirring, allowing sufficient time for formation of the colloidal particles. This was noted by the gradual color change from a colorless to a gray/green solution ~5 min after addition of the trisodium citrate. The flask was taken off the heat and cooled rapidly in an ice bath to quench any further reaction. Visible spectroscopy data characterizing the hydrosols[32] are detailed in Table 1.

Raman Microscopy. SERS spectra were collected using a Renishaw 2000 Raman microscope (Renishaw Plc., Old Town, Wotton-under-Edge, Gloucestershire, U.K.) with a low-power (24 mW) near-infrared 785-nm diode laser with power at the sampling point ~2 mW.[33,34] The instrument was wavelength calibrated with a silicon wafer focused under the 50× objective and collected as a static spectrum centered at 520 cm^{-1} for 1 s.

Samples were presented dried onto 15-mm-diameter polished CaF_2 disks with a single disk capable of holding six samples. Each sample was focused under a 50× objective and the motorized xy-stage programmed to take 50 spectra in a 10 × 5 grid within a ~1400 μm^2 area. Each spectrum was collected for 10 s. The next sample was then focused under the objective and the procedure repeated. For each study, four "biological replicates" were analyzed, meaning that samples were taken from four freshly prepared bacterial culture plates on different days and spectra collected as detailed above. An additional biological replicate was required to validate the results of the strain level discrimination (vide infra for details).

The GRAMS WiRE software package (Galactic Industries Corp., 395 Main St., Salem, NH) running under Windows 95 was used for instrument control and data capture. Stokes Raman spectra were collected as static spectra centered at 700 cm^{-1}, equating to a wavenumber range of 403.73−986.66 cm^{-1}. The resolution was ~6.5 cm^{-1}, and the bin size used was 1.015 cm^{-1}. Each sample was represented by a spectrum containing 575 points, and spectra were displayed in terms of the Raman scattered photon count (see Figure 1 for examples).

ASCII data were exported from the GRAMS WiRE software into Matlab version 6.1.0.450 release 12.1 (The Math Works, Inc., 24 Prime Par Way, Natick, MA). To address the problem of reproducibility relating to the SERS effect, the following procedure was performed for the analysis of the 21 isolates: (i) of the 50 spectra collected from each sample the 36 median spectra, with respect to the total Raman photon count, were extracted for further analysis; (ii) for each sample, the 36 spectra were added in order to increase S/N; (iii) next, the spectra were detrended by subtracting a linearly increasing baseline from 404 to 987 cm^{-1}; (iv) these spectra were then normalized so that the smallest photon count was set to 0 and the highest to +1 for each spectrum.

For the strain level discrimination experiment of *E. coli*, a similar series of processing algorithms was applied. Following extraction and summing of the median spectra, as described previously, the following procedure was carried out: (i) the spectra were normalized so that the smallest photon count was set to 0 and the highest to +1 for each spectrum; (ii) spectra were smoothed using a moving mean filter of width nine bins; (iii) the smoothed Savitzy−Golay[35] first-derivative spectra using nine-point smoothing were then taken for further analysis.

Cluster Analysis. Two models were generated by cluster analysis, one for genus-level *characterization* and the second for strain-level *discrimination* of seven *E. coli*. In the former we show that different isolates of the same species are clearly recovered together, and it was possible to draw comparisons between these clusters and traditional taxonomic associations. While discriminating between different *E. coli* strains, we show the good sensitivity of the technique and its potential application for the identification of microorganisms.

Cluster analysis was performed in Matlab as previously reported.[2,36] Briefly, principal components analysis (PCA[37]) was used to reduce the dimensionality of the SERS data prior to discriminant function analysis (DFA[38]). DFA then discriminated between groups on the basis of these retained PCs (the numbers used and the percentage explained variance are detailed in the figures) and the a priori knowledge of which spectra were the biological replicates. DFA was programmed to maximize the Fisher ratio (i.e., the within-class to between-class variance), and the spectral similarity between different classes reflects the optimal number of PCs that are fed into the DFA algorithm.[38] The number of PCs used for DFA were determined empirically because of the large spectral variation between the five different bacterial species analyzed, while we of course obeyed the parsimony principle[39] and extracted the fewest number of PCs that showed maximal class separation. The following protocol was adopted:

(1) All 84 SERS spectra from the 21 isolates were analyzed together. It was found that two groups (A and B) were clearly recovered in the first DF when eight PCs or more were used.

(33) Williams, K. P. J.; Pitt, G. D.; Batchelder, D. N.; Kip, B. J. *Appl. Spectrosc.* **1994**, *48*, 232−235.
(34) Williams, K. P. J.; Pitt, G. D.; Smith, B. J. E.; Whitley, A.; Batchelder, D. N.; Hayward, I. P. *J. Raman Spectrosc.* **1994**, *25*, 131−138.
(35) Savitzky, A.; Golay, M. J. E. *Anal. Chem.* **1964**, *36*, 1627−1633.
(36) Timmins, É. M.; Howell, S. A.; Alsberg, B. K.; Noble, W. C.; Goodacre, R. *J. Clin. Microbiol.* **1998**, *36*, 367−374.
(37) Jolliffe, I. T. *Principal Component Analysis*; Springer-Verlag: New York, 1986.
(38) Manly, B. F. J. *Multivariate Statistical Methods: A Primer*; Chapman & Hall: London, 1994.
(39) Seasholtz, M. B.; Kowalski, B. *Anal. Chim. Acta* **1993**, *277*, 165−177.

(2) The PC-DFA process was repeated on the spectra from group A containing *C. freundii*, *E. coli*, and *Klebsiella* spp. The cluster analysis showed two groups when a minimum of eight PCs were used. The first (A1) comprised only the *Citrobacter* and the second (A2) the *E. coli* and *Klebsiella* isolates (Figure 7A).

(3) The 10 bacteria in group A2 were analyzed on their own because of the close taxonomic relationship between *E. coli* and *Klebsiella*, which was reflected in their SERS spectra; 26 PCs were needed to recover each of the 4 replicates of each of the strains into separate clusters. Note of course that the resulting PC-DFA plot (Figure 7B) is not overtrained with this apparently high number of PCs.

(4) The PC-DFA process was repeated on the spectra from group B containing the *Enterococcus* spp. and *Proteus*. Fifteen PCs were needed to recover each of the four replicates of each of the strains into separate clusters, and two groups reflecting the different bacterial types were recovered.

Finally for the characterization exercise, the Euclidean distance between a priori group centers in DFA space was used to construct a similarity measure, and these distance measures were then processed by an agglomerative clustering algorithm to construct a dendrogram.[38] As detailed above, because of the differences in the similarities between the different bacteria, four PC-DFA models were produced. These were the combined in a "composite" dendrogram (Figure 7C) for ease of interpretation.

Validation for *E. coli* Isolate Identification. For the strain-level analysis of *E. coli* isolates, validation of the PC-DFA model was performed by the projection of a single biological replicate of each bacterial isolate into the PC-DFA space. This procedure has previously been reported in refs 40 and 41. Briefly, the first four biological replicates (see above for definition) of each isolate were used to construct a PC-DFA model as described above by performing PCA followed by DFA on *only the training set*. The test data from the fifth biological replicate, collected on a different day, were first projected into the PCA space and then the resultant PCs projected into the DFA space. The training and test clusters were then plotted on the same PC-DFA ordination plots for comparison. Finally, the resultant training set DFs and the projected DFs from the test set were used to construct a dendrogram by HCA as detailed above.

Scanning Electron Microscopy. An *E. coli* sample prepared for SERS was spotted and dried onto a Cambridge SEM specimen stub. Fifteen SERS spectra were captured from this sample and were very similar to all the others taken off CaF_2 (data not shown). For electron microscopy, the specimen was coated with 2 nm of platinum/palladium in an Agar high-resolution sputter coater fitted with a quartz thickness monitor. The images were acquired with a Hitachi S-4700 field emission scanning electron microscope operated in secondary electron ultra-high-resolution mode. The accelerating voltage was 4 kV, and the emission current was 10 μA with a 2-mm working distance.

RESULTS AND DISCUSSION

SERS Spectra. Figure 1 shows typical unprocessed spectra representing each of the six bacterial species isolated from UTI.

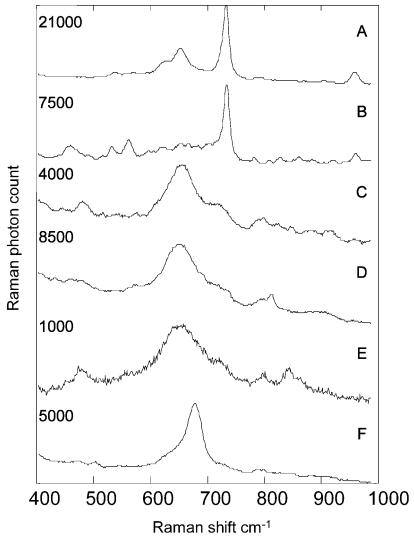

Figure 1. Typical unprocessed SERS spectra showing an example from each group of the UTI isolates. Each spectrum took 10 s to collect. (A) *Enterococcus* spp.; (B) *P. mirabilis*; (C) *E. coli*; (D) *K. pneumoniae*; (E) *K. oxytoca*; (F) *C. freundii*. The maximum Raman photon count for each spectrum is given on the left. Counts on the order of thousands and tens of thousands clearly indicate that these spectra result from the SERS process rather than normal Raman scattering.

The region between ~400 and ~980 cm^{-1} was chosen because preliminary studies revealed that this was the most information-rich area of the SERS spectrum. These spectra are easily discriminated with the naked eye, which suggests that there are significant differences in the (bio)chemistry between these organisms. Alternatively these variations could be due to the nature of the SERS process, where the same analyte in a chemically heterogeneous bacterium cannot be expected to repeatedly satisfy all of the criteria for SERS, namely, orientation, and presence within the range of the enhanced local optical field.

To investigate this further and to demonstrate that reproducible SERS fingerprints could be obtained using *different* batches of colloidal silver solution, spectra of a single *E. coli* isolate (Eco17) and a single isolate of the *Enterococcus* sp. (EntC90) were obtained (Figure 2A) with the three hydrosols characterized in Table 1. Despite varying signal intensities, the spectra do exhibit clear similarities. However, on closer inspection, there are subtle quantitative differences in these "raw" spectra that need to be accounted for before SERS can be used within the context of "whole-organism fingerprinting".

This problem of absolute replication of SERS spectra is akin to MALDI-MS where the dried sample−matrix preparation is inhomogeneous, requiring the selection of "sweet" spots on the target that would give the best ion formation.[4] In MALDI-MS, this challenge is overcome by coadding individual spectra. We have adopted a similar approach to achieve reproducible SERS spectra that are representative of the sample being studied, where, as detailed above, the 36 median spectra (with respect to photon count) are added together. To see the effect of this preprocessing step, representative spectra from an *Enterococcus* isolate and *E. coli* isolate are shown in panels B and C of Figure 2, respectively. It can clearly be seen that these spectra have significant qualitative similarities compared to the "raw" unprocessed spectra (Figure 2A).

(40) Radovic, B. S.; Goodacre, R.; Anklam, E. *J. Anal. Appl. Pyrolysis* **2001**, *60*, 79−87.
(41) Kaderbhai, N. N.; Broadhurst, D. I.; Ellis, D. I.; Goodacre, R.; Kell, D. B. *Comp. Funct. Genomics* **2003**, *4*, 376−391.

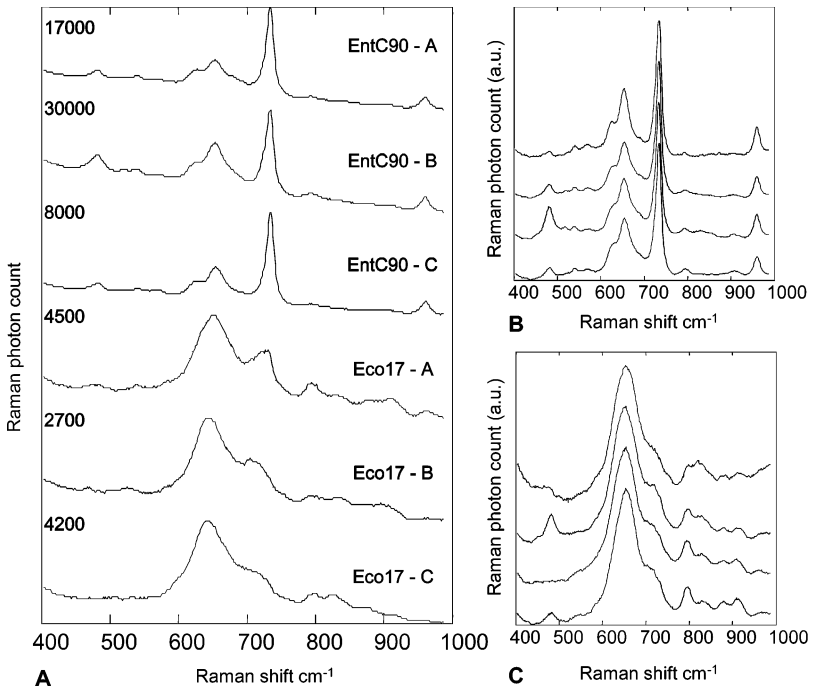

Figure 2. (A) SERS spectra representing an *Enterococcus* sp. (EntC90) and *E. coli* (Eco17) taken using aggregated colloidal silver solutions from three separate batch preparations (A−C), as detailed in Table 1. Maximum Raman photon counts for each sample are given to the left of the figure. For the three spectra of each isolate, clear similarities can be seen with the naked eye, indicating that reproducibility can be achieved even when using different batches of colloidal solution. (B) Processed enterococci spectra of each of the four EntC90 replicates used in the characterization study. In comparison to the raw spectra in (A), these show far greater qualitative and quantitative similarities, particularly in the 600−1000-cm^{-1} wavenumber shift region. (C) Processed *E. coli* spectra of the Eco17 isolate used in the characterization of UTIs. As noted in (B), these spectra are virtually identical.

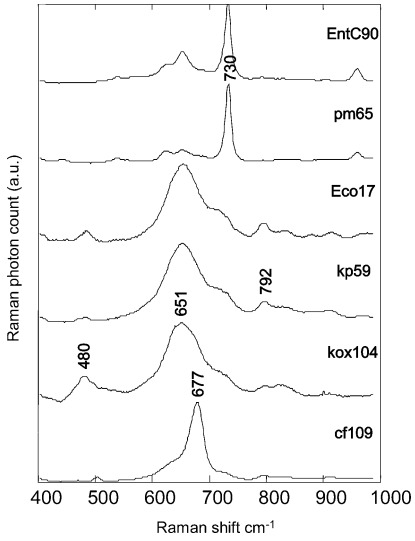

Figure 3. Processed SERS spectra of UTI isolates. Details of the method used are given in the text. EntC90, *Enterococcus spp.*; pm65, *P. mirabilis*; Eco17, *E. coli*; kp59, *K. pneumoniae*; kox108, *K. oxytoca*; and cf109, *C. freundii*. The wavenumbers of some of the main bands are included.

Typical processed SERS spectra are shown in Figure 3. The similarity between the spectra of the two *Klebsiella* spp. and *E. coli* might be expected since all are Gram-negative facultative anaerobic rods, although on closer inspection, some differences can be observed, particularly in the region of the 480- and the 800-cm^{-1} shift. *Citrobacter* exhibits sharp peak at 677 cm^{-1}, attributable to an extracellular L-cysteine-rich polypeptide toxin produced by the organism.[42,43]

The spectra of the enterococci and *Proteus* are extremely interesting. Considering the vast difference in their cell envelope biochemistry (*Proteus* are Gram-negative yet *Enterococcus* are Gram-positive) and that the colloid will be in intimate contact with the outer cell wall, the assumption would be that these spectra should be quite different. By contrast, these spectra share several key features. The main feature is a sharp peak at ∼730 cm^{-1}, which although present in the other spectra is of much lower magnitude. This peak may be attributable to polysaccharide structures, since the cell walls of *Enterococcus* spp. are formed from peptidoglycan, which is rich in *N*-acetyl-D-glucosamine (NAG) and *N*-acetylmuramic acid. NAG is also present on the cell surface of *Proteus*, where it is produced as a component of an acidic capsular polysaccharide.[44] Raman spectra of NAG collected in this laboratory did not exhibit a peak at this wavenumber shift (data not shown); however, Raman peaks in this region from microbes have been attributed to vibrational modes of polysaccharides.[45] The SERS spectrum of NAG taken in this laboratory (Figure 4) shows an intense peak at 730 cm^{-1}, which suggests for *Enterococcus* and *Proteus* that NAG is the contributing chemical species. It is likely that this peak can be assigned to a glycosidic ring mode, since the SERS spectrum of D-glucose (Figure 4) also exhibits a

(42) Gest, H. *Microbiol. Today* **1999**, *26*, 70−72.
(43) McCreery, R. L. Thermo Galactic; http://spectra.galactic.com/SpectraOnline/, 2001; Vol. 2002.
(44) Moat, A. G.; Foster, J. W. *Microbial Physiology*, 3 ed.; Wiley: New York, 1995.
(45) Maquelin, K. Ph.D. Erasmus Universiteit, Rotterdam, 2002.

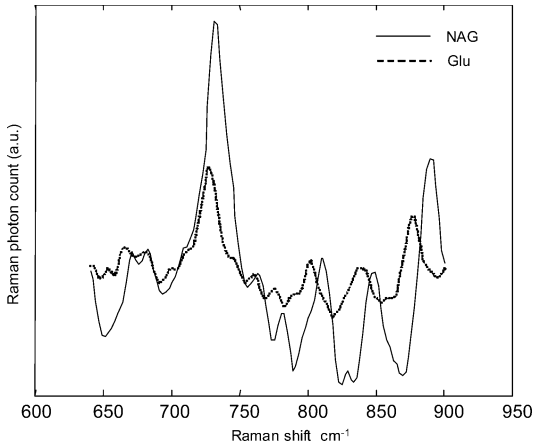

Figure 4. SERS spectra of *N*-acetyl-D-glucosamine (NAG) and D-Glucose (Glu). The most intense peak at ~730 cm^{-1} is likely to be due to a vibrational mode of the glycosidic ring.

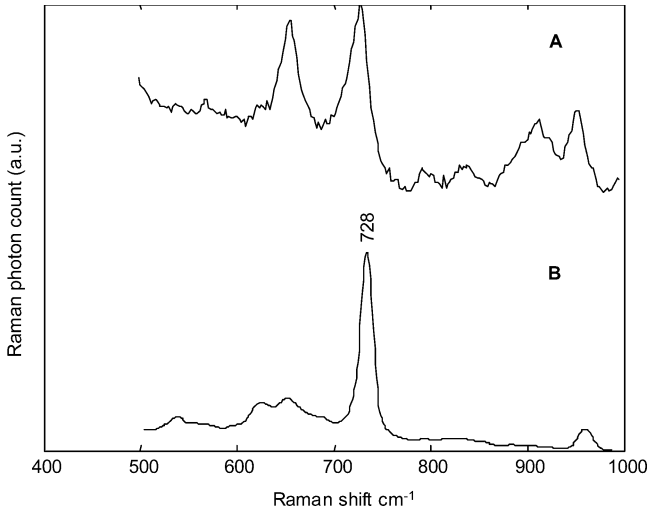

Figure 5. SERS spectrum of the supernatant from washed and spun *P. mirabilis* (A) compared to that of *P. mirabilis* cells (B). The spectra share an intense peak in the ~730-cm^{-1} region, which is most likely a contribution from carbohydrate species.

peak at ~730 cm^{-1}. SERS analysis of the supernatant from washed and spun *Proteus* cells (Figure 5) also produced a spectrum with a strong band at 728 cm^{-1}. While there is a slight shift in this band, in solution these capsular polysaccharides would be likely to exhibit alternative conformational modes; thus, one would expect differences in SERS spectra between *Proteus* cells and the supernatant.

While there is the potential to gain chemical information from these SERS spectra, they are difficult to interpret. There could be any number of SERS-active vibrational modes present in biochemically complex samples such as bacteria. In this case, with a priori information on the biochemistry of the organisms studied, it is possible to target investigations into certain peaks; however, at best any peak assignments can only be tentative. A problem also arises from the lack of a database resource of SERS spectra, making the process of peak identification more time-consuming. Although resources for standard Raman spectra of biological materials are slowly becoming available and can be useful, it is not always the case that peaks expressed in a Raman spectrum will also be observed in the SERS spectrum of the same sample.

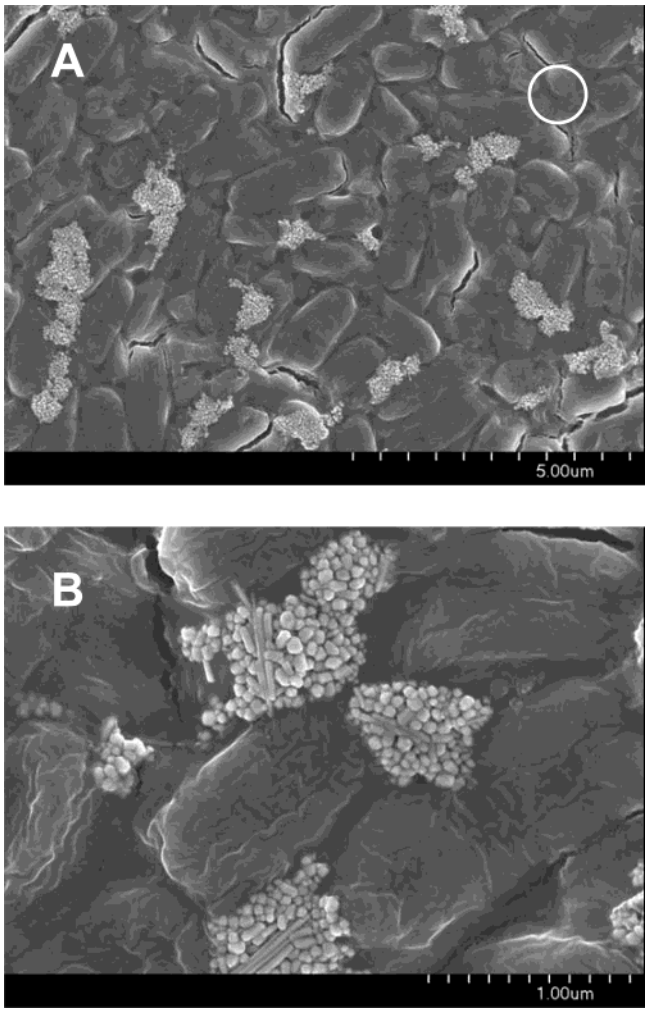

Figure 6. (A) SEM image of *E. coli* and aggregated silver colloid, prepared for SERS. The approximate laser spot size is denoted by the circle outlined in white. Since the cells do not appear to have lysed, the shifts observed in the SERS spectra are a product of cell wall biochemistry or other chemical components external to the cell. (B) A higher magnification image of *E. coli* and colloidal silver aggregates. The heterogeneity in size and shape of the colloidal silver particles can clearly be seen.

Scanning Electron Microscopy. Figure 6A shows a scanning electron micrograph (SEM) image of an *E. coli* sample prepared for SERS. The microbes can be clearly identified as the dark rod-shaped structures approximately 1−2 μm in length and the aggregated silver colloids as the lighter mostly spherical structures. It is evident that the size and dispersion of the aggregated colloids is quite heterogeneous and given the size of the laser spot helps explain the unpredictability of hitting SERS "sweet" spots when a metal substrate is used under these conditions. The higher magnification image in Figure 6B shows details of the orientation of the microbial cell wall with respect to the aggregated colloid. Since the cells do not appear to have lysed, this suggests that the shifts observed in the SERS spectra are a product of cell wall biochemistry or other chemical components external to the cell.

The morphology of the colloidal particles (Figure 6B) is notable as there are a variety of sizes and shapes: rods, spheres, and spheroids ranging from ~30 to 300 nm. This is characteristic of citrate-reduced silver colloids produced under a batch process.[26]

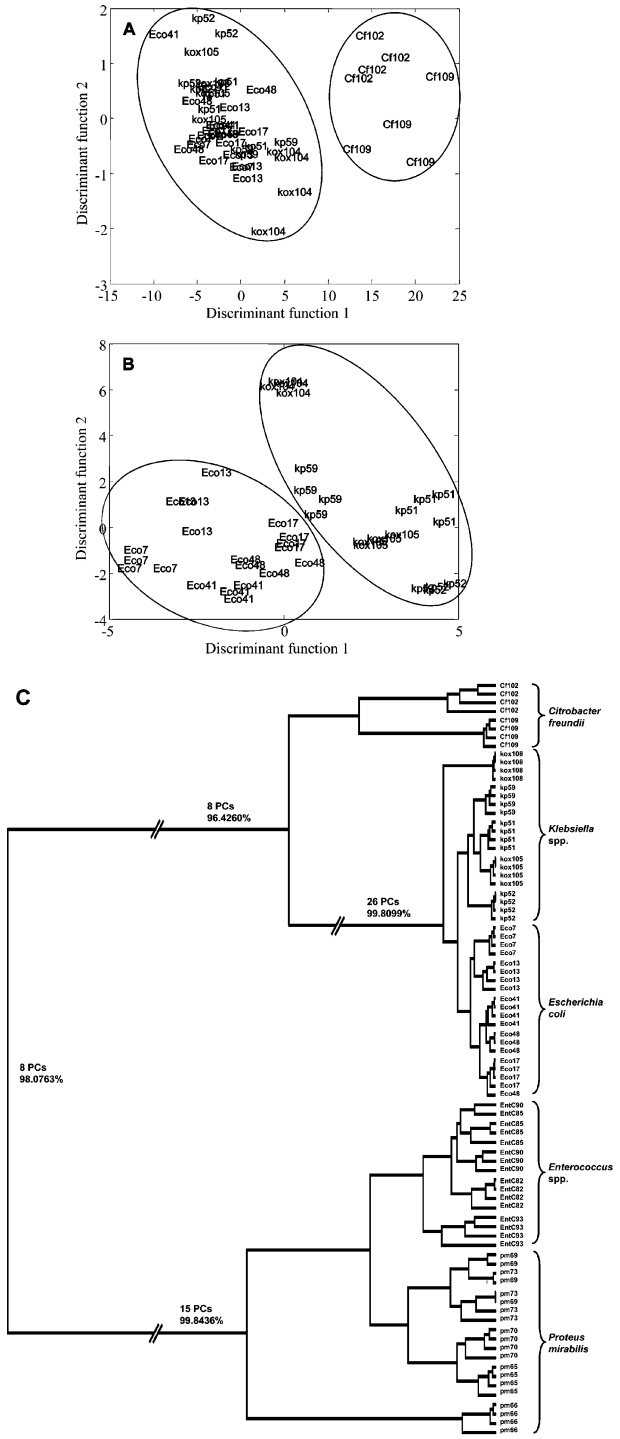

Figure 7. (A) PC-DFA ordination plot showing clusters obtained from the analysis of *Citrobacter*, *E. coli*, and *Klebsiella* isolates used in characterization of the UTI bacteria. The strategy for the analysis is explained in the text. *Citrobacter* can be seen to be clearly separated from *E. coli* and *Klebsiella* along the first discriminant function. (B) A further example of an ordination plot produced by the same analysis for the *E. coli*, *Klebsiella* subgroup. Although 26 PCs were used to recover these clusters, it is clear that the resultant model is not subject to overtraining. (C) A composite dendrogram derived from hierarchical cluster analysis utilizing the PC-DFA space (including the results in (A) and (B)) resulting from the protocol followed in the text. Full details of the number of PCs used at each level (boundaries indicated by parallel diagonal lines) and the associated percentage explained variance is provided. This dendrogram allows for the easy interpretation of taxonomic associations between these UTI bacteria.

Since the observation of SERS due to the electromagnetic effect is dependent on the size and shape of these particles, it is clear that the ability to reproduce spectra will also be affected by the lack of a uniform SERS substrate and hence why we adopted the process of taking 50 SERS spectra at random locations on the target and then only using the 36 median spectra from these.

Cluster Analysis. Using results from the characterization study, a composite dendrogram (Figure 7C) was generated by HCA as described above. Due to significant differences between spectra, cluster analyses were performed sequentially as detailed earlier in the text. For clarity, example DFA ordination plots are also shown in Figure 7A and B, which clearly demonstrate why it was necessary to extract subsets of data to perform an analysis unbiased by large intergroup distances, a process adopted by us and others for the analysis of spectroscopic data.[5,45] The resultant dendrogram shows clear characterization at the genus level for each of the groups analyzed.

The relationship shown between the *Proteus* and *Enterococcus* is not unsurprising given the similarity in cell surface chemistry discussed above. The pm66 isolate stands out, forming a subgroup of its own. Reviewing the spectra (data not shown) one can see that although the same peaks are present for pm66 as for the other *Proteus* isolates, the relative magnitudes of these peaks are different, with the 651- and 730-cm^{-1} bands having a similar size. This indicates that the acidic capsular polysaccharide coating of this microorganism in some way exhibits a chemical structure diverse from that of the other *Proteus* isolates studied.

To investigate the potential of SERS to discriminate to the strain level, seven isolates of *E. coli* were selected for study by this technique. The ordination plots in Figure 8A and B show the results from the validation process described above. That the test spectra are projected within the clearly defined clusters for each of the isolates studied undoubtedly shows that SERS does provide the sensitivity and reproducibility for subspecies discrimination. To illustrate this further, a composite dendrogram was also produced from these cluster analyses (Figure 8C), where it can be seen that the projected SERS spectra (marked with an asterix) fall within the training data used to construct the dendrogram. These isolates were previously studied by Kassama et al.[30] using the genetic fingerprinting technique of amplified fragment length polymorphism (AFLP). The results produced by AFLP and SERS are largely comparable, which is highly encouraging given that SERS interrogates the cell surface chemistry while AFLP the DNA.

CONCLUSION

SERS is recognized as a method for increasing the Raman cross section of a sample under analysis/interrogation, but has been generally considered to have poor reproducibility with respect to relative signal intensities, and so has been limited to the detection of substances in low concentrations. The problem of spectral reproducibility is overcome by the simple averaging of selected spectra, a process widely adopted within the analysis of biological materials using MALDI-MS. While other workers have explored SERS for the characterization of bacteria, none of these studies has shown that bacteria can be discriminated by their SERS spectra. By contrast, this study clearly demonstrates the potential for SERS to produce spectra that can be used for rapid whole-organism fingerprinting, and in conjunction with simple cluster analyses, such hyperspectral data can be used to

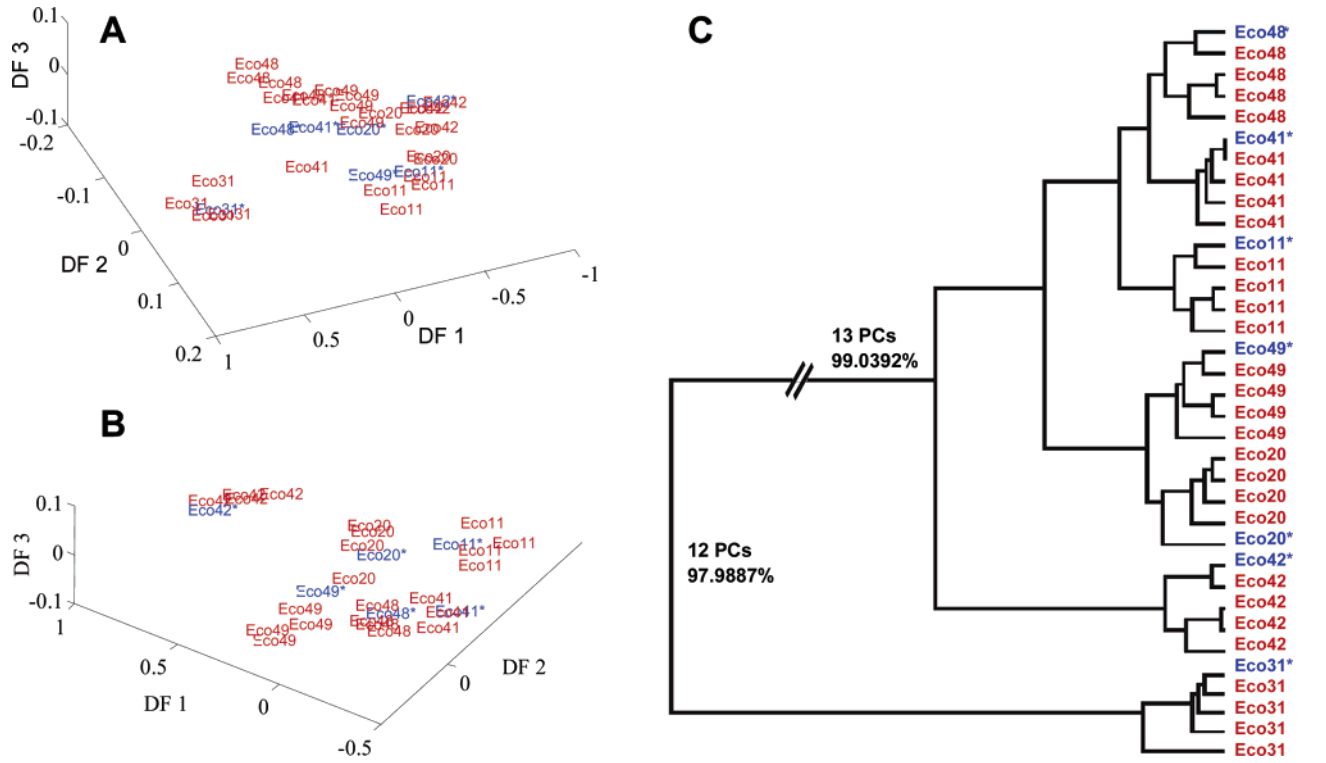

Figure 8. (A) Ordination plot characterizing seven clinical isolates of *E. coli* from UTIs. The entries in red represent the training data and those marked with an asterisk in blue, the validation data. The analysis was performed and validated as described in the text. Isolate Eco31 can be seen to form a cluster apart from the rest of the isolates. Therefore, Eco31 was extracted and the remaining isolates analyzed again. This result (B) clearly demonstrates that SERS can be applied to discrimination of microorganisms at the strain level. (C) A composite dendrogram generated by HCA using the combined PC-DFA space from the training and validation replicates used to generate the ordination plots in (A) and (B). This representation of the results shows how the validation replicates fall tightly within the clusters formed from the training data.

discriminate between microorganisms to the strain level. We believe that SERS presents itself as a complementary whole-organism fingerprinting approach for the rapid characterization of bacteria.

ACKNOWLEDGMENT

R.M.J. is indebted to Renishaw Plc. and the U.K. EPSRC for his CASE Ph.D. studentship. Special thanks to Dr. Stephen C. Wade for the SEM images. R.G. also thanks the U.K. BBSRC Engineering and Biological Systems Committee for financial support.

Received for review June 25, 2003. Accepted October 7, 2003.

AC034689C